AT03-76SF 70038

THIRD QUARTERLY PROGRESS REPORT

APRIL 1, 1975 - JUNE 30, 1975

SUBGRAIN REFINEMENT STRENGTHENING

Sponsored by

Advanced Fuel Systems Branch,
Division of Reactor Research and Development
USERDA
Washington, D.C. 20545

Contract AT(04-3) - 326-PA#38

prepared by

Rodney Klundt, Yoshio Monma and Oleg D. Sherby

MASTER

Department of Materials Science and Engineering
Stanford University
Stanford, California 94305

ABSTRACT

The possible influence of subgrain size on the creep strength of 304 stainless steel was assessed by constant crosshead speed tests at 900, 1000 and 1100°C. The data obtained were compared with the results of other investigations. It appears that 304 stainless steel can be strengthened considerably by the presence of subgrains. Specifically, the flow stress, σ, is shown to be a function of the subgrain size, λ, following the relation $\sigma \propto \lambda^{-0.35}$. It is predicted that 304 stainless steel can be increased in strength by a factor of 2.7 over the normally expected strength at 650°C and $\dot{\varepsilon} = 10^{-10}\ S^{-1}$ (i.e. one year rupture life) if stable subgrains 0.2μm in size can be developed. Decrease in strain-rate tests reveal the possible instability of subgrains in 304 stainless steel at high temperatures. Future studies will be devoted to understanding and controlling these instabilities.

INTRODUCTION

During the period January to June 1975 we attempted to determine the influence of subgrain size on the creep strength of 304 stainless steel. Preliminary studies were also performed on 316 and 321 austenitic stainless steels, a ferritic stainless steel (E-Brite 26-1), and Nimonic PE-16. In this quarterly progress report we will only describe the results obtained on the 304 austenitic stainless steel.

MATERIALS AND EXPERIMENTAL TECHNIQUES

The stainless steel studied was prepared in the form of round circular cylinders, 0.48" in diameter and .72" long. The samples were machined from 304 stainless steel rods received in the as-cold-worked state. Since all the tests were performed at 900, 1000 and 1100°C it was assumed that the prior cold worked condition was eliminated during annealing at the test temperature (30 minutes soaking time) prior to compression testing. The grain size was ASTM 6 (.04 mm diameter). Constant crosshead speed tests were performed at rates varying from 0.2" per minute (4.6×10^{-3} S^{-1}) to .0005" per minute (1.2×10^{-5} S^{-1}). The chemical composition of the 304 stainless steel is given in Table 1; we also list the chemical composition of a precipitation hardened stainless steel 304H (a Japanese steel) for which extensive creep data is available[1].

The stainless steel was studied by two different types of mechanical tests. One method was to deform the material at constant crosshead speed to large strains (true strain of about 0.5). These tests permitted us to determine the steady state flow characteristics of 304 stainless steel as a function of temperature and strain rate. The second method was to perform strain-rate-change tests in order to assess the possible influence of subgrain size on the creep strength of the 304 stainless steel.

Table 1A

Chemical Composition of 304 Stainless Steel

Material	C	Si	Mn	P	S	Cr	Mo	Ni	Al	N
304*	0.055	0.55	1.79	0.054	0.025	18.13	0.49	8.5	--	--
304H** (ABE)	0.08	0.55	1.43	0.021	0.010	19.3	0.04	9.5	0.014	0.026

* This study; compression tests

** Tensile creep

Table 1B

Mechanical Properties at Room Temperature

Material	0.2% YS ksi	0.2% YS MPa	UTS ksi	UTS MPa	Elong (%)	R.A. (%)	R_B hardness	Grain Size (ASTM)
304	72.9	486	100.8	672	46	74	95	6.3
304H* (ABE)	39.8	265	92.7	618	72	84	81	5.1

*ABE is a heat number in NRIM creep data sheet No. 4

In our present analysis of the behavior of stainless steel we made the assumption that strain hardening of this material at elevated temperature is due primarily to the formation of subgrains. That is, subgrain formation is the dominant structural change occurring during plastic deformation and subgrain boundaries are the principal barriers leading to the strengthening observed during plastic flow*. We utilized the following equation to assess quantitatively the subgrain size - creep strength relationship:

$$\dot{\varepsilon} = S\ \lambda^{p}\ \sigma^{N} \qquad (1)$$

Here $\dot{\varepsilon}$ is the creep rate, λ is the subgrain size, σ is the creep stress and S, p and N are material constants. The stress exponent N is obtained by performing strain-rate-change tests at constant structure. Thus, one can write, for the case where structure is constant (i.e. λ = constant),

$$N\Big|_{\lambda} = \frac{\ln \dot{\varepsilon}_{2}/\dot{\varepsilon}_{1}}{\ln \sigma_{2}/\sigma_{1}} \qquad (2)$$

Here σ_1 and σ_2 are the values of the flow stress immediately before and immediately after a change in strain rate ($\dot{\varepsilon}_1$ and $\dot{\varepsilon}_2$ respectively).

The subgrain size exponent, p, can be determined from a knowledge of the value of N and the steady state flow stress-strain rate relationship. We illustrate the basis of the calculation by the following discussion. When one deals with steady state involving either a steady state creep rate (at constant stress) or a steady state flow stress (at constant strain rate) one must consider the variation of the subgrain size with the flow stress[2]. It is well established[3] that λ takes on the following relation with the flow stress for

---

* Other factors such as solute-dislocation interactions and grain boundary sliding can also influence the creep rate. As our understanding of these factors evolves we will consider them in our studies on subgrain strengthened alloys.

many polycrystalline materials:

$$\lambda = Ab \left(\frac{\sigma}{E}\right)^{-m} \tag{3a}$$

In this relation b is burgers vector, E is Young's modulus and A and m are material constants. At values of σ/E below about 2×10^{-3}, m is equal to unity for most polycrystalline materials and A is about equal to 4[3]. (At high values of σ/E, m is equal to about two and A equals 10^{-2})[3]. Our studies on 304 stainless steel were restricted to strain rates and temperature which yielded values of $\frac{\sigma}{E}$ below 2×10^{-3}. Under these conditions equation (3a) reduces to the following at a given temperature:

$$\lambda = C\,\sigma^{-1} \tag{3b}$$

Substituting this relation into equation (1) for the case of steady state flow conditions one obtains

$$\dot{\varepsilon}_s = S'\,\sigma^{(N-p)} = S'\,\sigma^{n} \tag{4}$$

where $S' = SC^p$ and n, the normally obtained stress exponent for creep flow is equal to (N-p). The parameter, n, is, of course, calculated readily from steady state creep rate data using the following relation

$$n = \frac{\ln\left[(\dot{\varepsilon}_s)_2/(\dot{\varepsilon}_s)_1\right]}{\ln \sigma_{3/\sigma_1}} \tag{5}$$

where $(\dot{\varepsilon}_s)_2$ and $(\dot{\varepsilon}_s)_1$ are the steady state creep rates at the corresponding creep stresses σ_3 and σ_1 (see Figure 1). From equation (4) we thus see that the parameter p is obtainable from the following relation:

$$p = (N-n) \tag{6}$$

Figure 1 graphically illustrates the method that was used to obtain the parameters N and n, and therefore p, from a <u>single</u> experiment using a change-in-strain-rate technique. In our studies on 304 stainless steel N values were

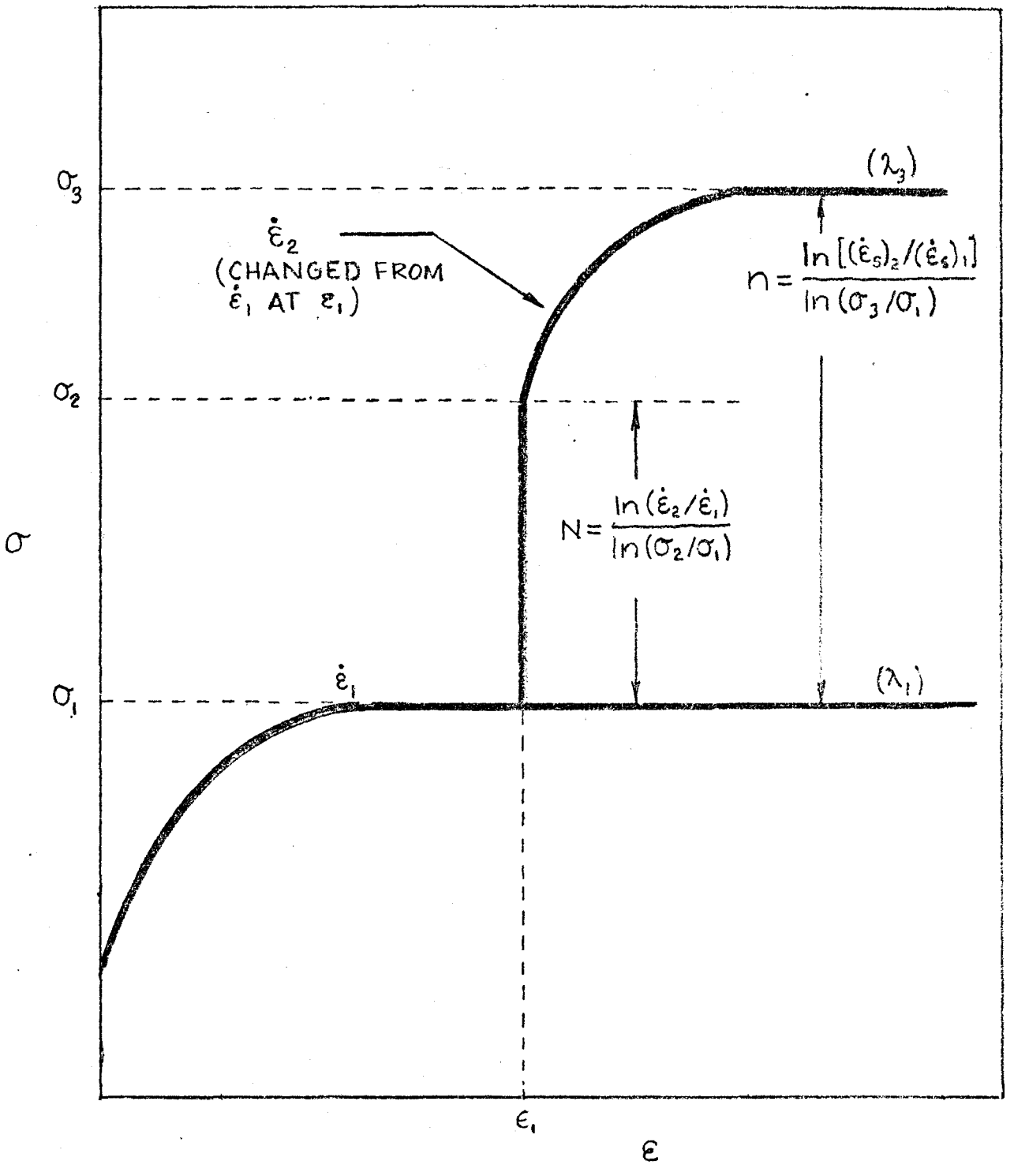

Figure 1. Schematic diagram of a change-in-strain-rate test illustrating the method of determining the stress exponent, N, at constant structure and the stress exponent, n, for steady state structures.

determined by the change-in-strain-rate method; furthermore, we compared our results with those calculated from the published data of Barraclough and Sellars[4] and of Cuddy[5]. The values of n were determined from knowing the relation between the steady state flow stress and the strain rate.

RESULTS

Results of the steady state flow stress-strain rate relation for 304 stainless steel are given in Table 2. Tests were performed at 900, 1000 and 1100°C over one order of magnitude of σ/E values (2×10^{-4} to 2×10^{-3}). Figure 2 illustrates the results showing the power law range of creep ($n \simeq 5$) and power law breakdown at $\sigma/E \simeq 10^{-3}$. This is typical of the behavior of most pure polycrystalline solids[6]. From these results values of n can be determined at any given value of σ/E and temperature.

Typical results of change-in-strain-rate tests are given in Figure 3 at 1100°C. A summary of the change-in-strain-rate tests is given in Table 3. Only increase in strain-rate-tests are reported; anomalous results were obtained at 1100°C for decrease-in-strain-rate tests and these will be discussed later.

Change-in-strain-rate tests were performed by Barraclough and Sellars[5]. They performed their tests in torsion and a typical result from their work is shown in Figure 4. They did not analyze their data in the manner developed here but it was possible for us to deduce N and n values for the single example they gave (reproduced here as Figure 4). Cuddy performed stress-drop tests on 304 stainless steel (equivalent to a decrease-in-strain-rate test) and typical results from this investigation is shown in Figure 5. Such tests permit us to calculate N values since the strain rate-stress relation shown is obtained at constant structure.

All the values of N and n calculated from this investigation and from the data of Barraclough and Sellars, as well as Cuddy, are given in Figure 6. It

Table 2

Compression Creep Data for 304 Stainless Steel

Specimen	Temp.	$\dot{\varepsilon}(sec^{-1})$	$\dot{\varepsilon}/D_L$	σ/E	σ, ksi (ε = 0.35)
SSC-11	900	$6.6x10^{-2}$	$5.12x10^{11}$	$1.80x10^{-3}$	30.7
SSC-3		$6.6x10^{-3}$	$5.12x10^{10}$	$1.47x10^{-3}$	25.1
SSC-6		$6.6x10^{-3}$	$5.12x10^{10}$	$1.57x10^{-3}$	26.8
SSC-1		$6.6x10^{-4}$	$5.12x10^{9}$	$1.12x10^{-3}$	19.2
SSC-2		$6.6x10^{-5}$	$5.12x10^{8}$	$8.71x10^{-4}$	14.9
SSC-42		$6.6x10^{-5}$	$5.12x10^{8}$	$7.87x10^{-4}$	13.5
SSC-16		$3.3x10^{-5}$	$2.56x10^{8}$	$7.66x10^{-4}$	13.1
SSC-17		$6.6x10^{-6}$	$5.12x10^{7}$	$4.80x10^{-4}$	8.2
SSC-39		$6.6x10^{-6}$	$5.12x10^{7}$	$4.91x10^{-4}$	8.6
SSC-37	1000	$6.6x10^{-4}$	$5.36x10^{8}$	$7.60x10^{-4}$	11.4
SSC-41		$6.6x10^{-4}$	$5.36x10^{8}$	$7.23x10^{-4}$	10.8
SSC-33		$1.6x10^{-4}$	$1.30x10^{8}$	$5.33x10^{-4}$	8.0
SSC-36		$6.6x10^{-5}$	$5.36x10^{7}$	$4.27x10^{-4}$	6.4
SSC-31		$1.6x10^{-5}$	$1.30x10^{7}$	$3.13x10^{-4}$	4.7
SSC-32	1100	$7.3x10^{-3}$	$8.70x10^{8}$	$7.31x10^{-4}$	9.5
SSC-44		$6.6x10^{-3}$	$7.87x10^{8}$	$6.58x10^{-4}$	8.55
SSC-27		$6.6x10^{-4}$	$7.87x10^{7}$	$4.54x10^{-4}$	5.9
SSC-43		$6.6x10^{-4}$	$7.87x10^{7}$	$4.54x10^{-4}$	5.9
SSC-29		$1.6x10^{-4}$	$1.91x10^{7}$	$3.38x10^{-4}$	4.4
SSC-38		$1.6x10^{-4}$	$1.91x10^{7}$	$3.38x10^{-4}$	4.4
SSC-30		$6.6x10^{-5}$	$7.87x10^{6}$	$2.92x10^{-4}$	3.8
SSC-35		$1.6x10^{-5}$	$1.91x10^{6}$	$2.13x10^{-4}$	2.8

Table 3

Summary of Strain-Rate Change Test Data for 304 Stainless Steel

Specimen	Temp. °C	Strain Rate at ε=0.35 sec^{-1}		Stress ksi			$\frac{\lambda}{b} \approx 4(\frac{\sigma}{E})^{-1}$		Stress Exponents		p = N-n	$\frac{p}{N}$
		$\dot{\varepsilon}_1$	$\dot{\varepsilon}_2$	σ_1	σ_2	σ_3	σ_1/E	λ μm	N	n		
SSC-42	900	6.57×10^{-5}	6.57×10^{-4}	13.32	16.5-16.9	17.98	7.8×10^{-4}	1.3	9.7-10.8	7.7	2.0-3.0	.20-.28
SSC-39		6.57×10^{-6}	1.64×10^{-4}	8.93	13.1-13.5	14.43	5.2×10^{-4}	1.9	7.8-8.4	6.7	1.1-1.7	.1 20
SSC-37	1000	6.57×10^{-4}	6.57×10^{-3}	11.37	13.8-14.3	16.05	7.6×10^{-4}	1.3	10.0-11.9	6.7	3.3-5.2	.33-.44
SSC-33		1.64×10^{-4}	6.57×10^{-4}	8.06	9.2- 9.4	10.53	5.4×10^{-4}	1.8	9.1-10.6	5.2	3.9-5.4	.43-.51
SSC-36		6.57×10^{-5}	6.57×10^{-4}	6.46	8.3-8.6	10.31	4.3×10^{-4}	2.3	8.0-9.2	4.9	3.5-5.5	.44-.60
SSC-31		1.64×10^{-5}	6.57×10^{-4}	4.70	7.4-8.0	9.56	3.1×10^{-4}	3.2	6.7-7.8	5.2	1.5-2.6	.22-.33
SSC-27	1100	6.57×10^{-4}	6.57×10^{-3}	5.97	7.5-7.8	9.31	4.6×10^{-4}	2.2	8.6-10.1	5.2	3.4-4.9	.40-.48
SSC-29		1.64×10^{-4}	6.57×10^{-4}	4.31	5.1-5.3	5.78	3.2×10^{-4}	3.1	6.7-8.2	4.7	2.0-3.5	.29-.43
SSC-30		6.57×10^{-5}	6.57×10^{-4}	3.72	5.0-5.2	5.92	2.8×10^{-4}	3.6	6.9-7.8	5.0	1.9-2.8	.27-.36
SSC-35		1.64×10^{-5}	6.57×10^{-4}	2.72	4.3-4.7	5.86	2.1×10^{-4}	4.8	6.7-8.0	4.8	1.9-3.2	.2^ 42

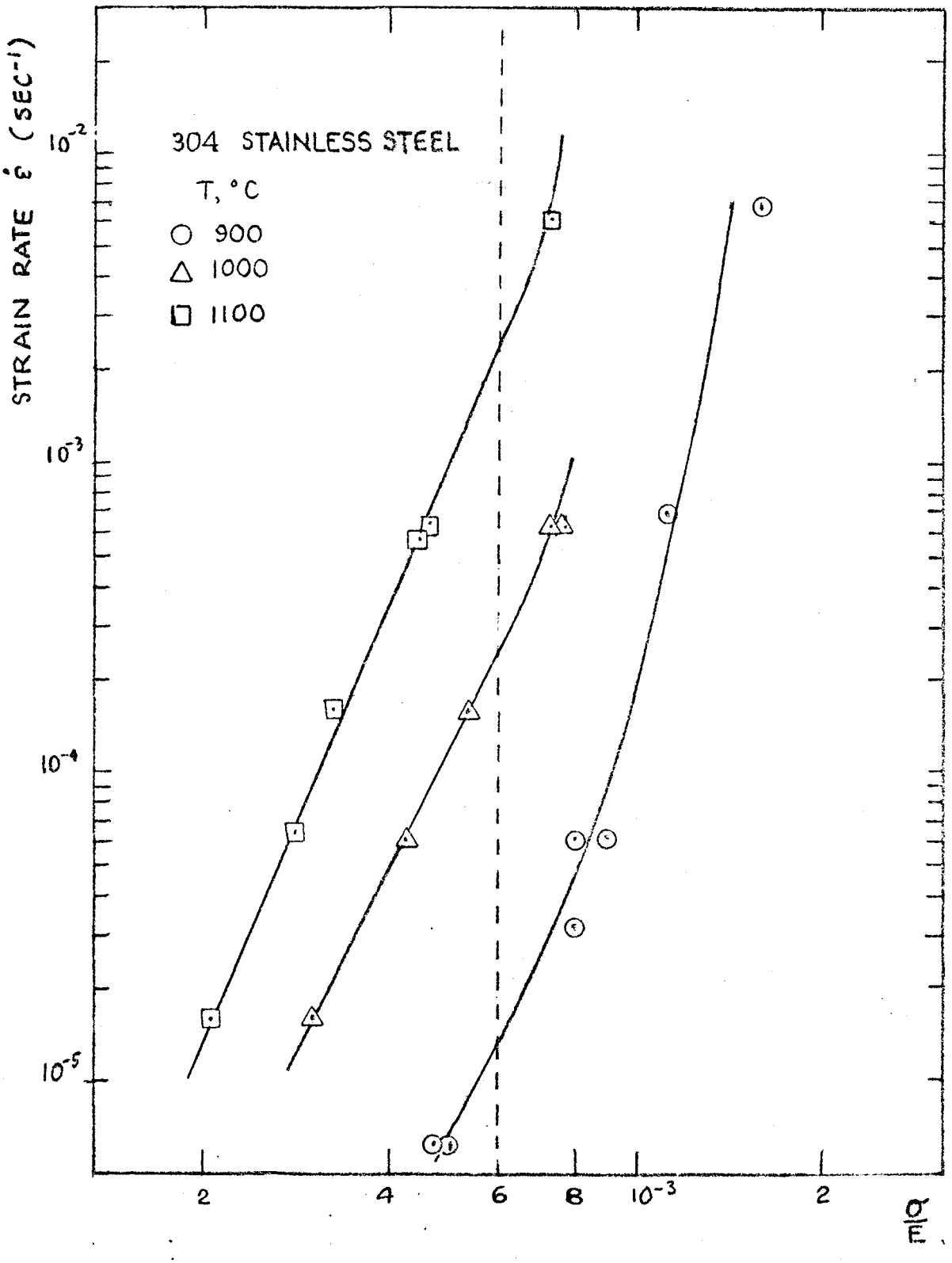

Figure 2. Influence of strain rate on the modulus compensated steady state flow stress for 304 stainless steel. Tests were performed in compression at 900, 1000 and 1100°C.

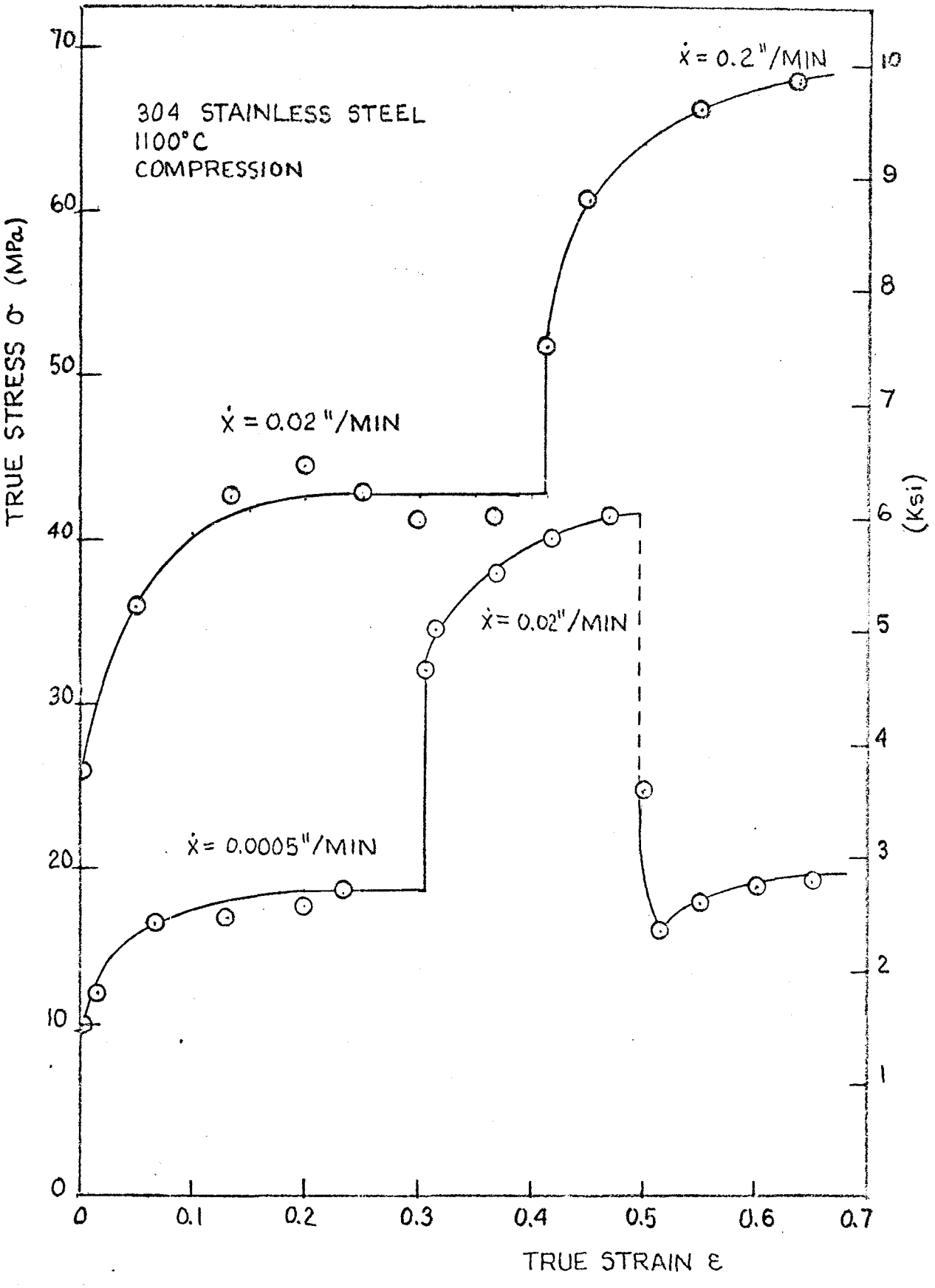

Figure 3. Typical strain-rate change tests for 304 stainless steel at 1100°C.

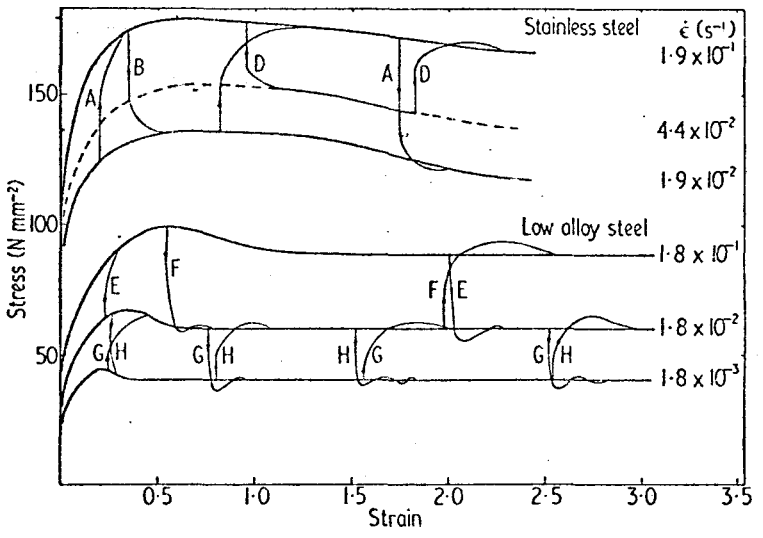

Figure 4. Change-in-strain-rate tests performed in torsion at 932°C on 304 stainless steel (upper curves). Data of Barraclough and Sellars[4].

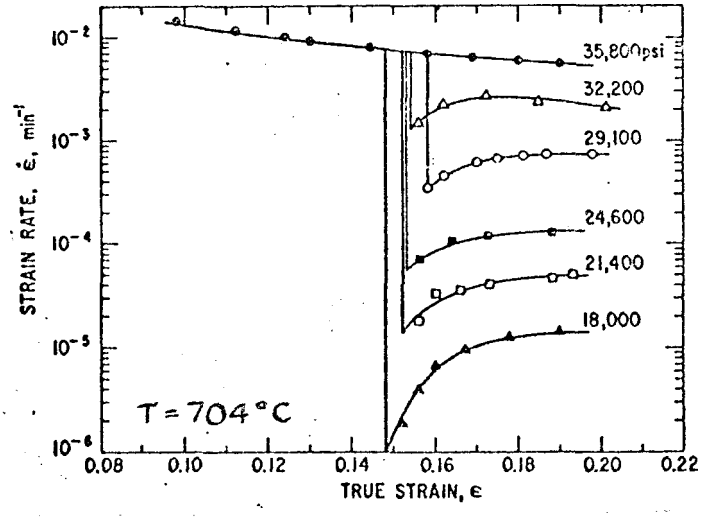

Figure 5. Change in stress creep tests (stress drop creep tests) on 304 stainless steel illustrating the influence of creep stress on the corresponding creep rate at constant structure. Such tests permit calculation of the stress exponent, N, as well as the normal stress exponent n. Data of Cuddy[5].

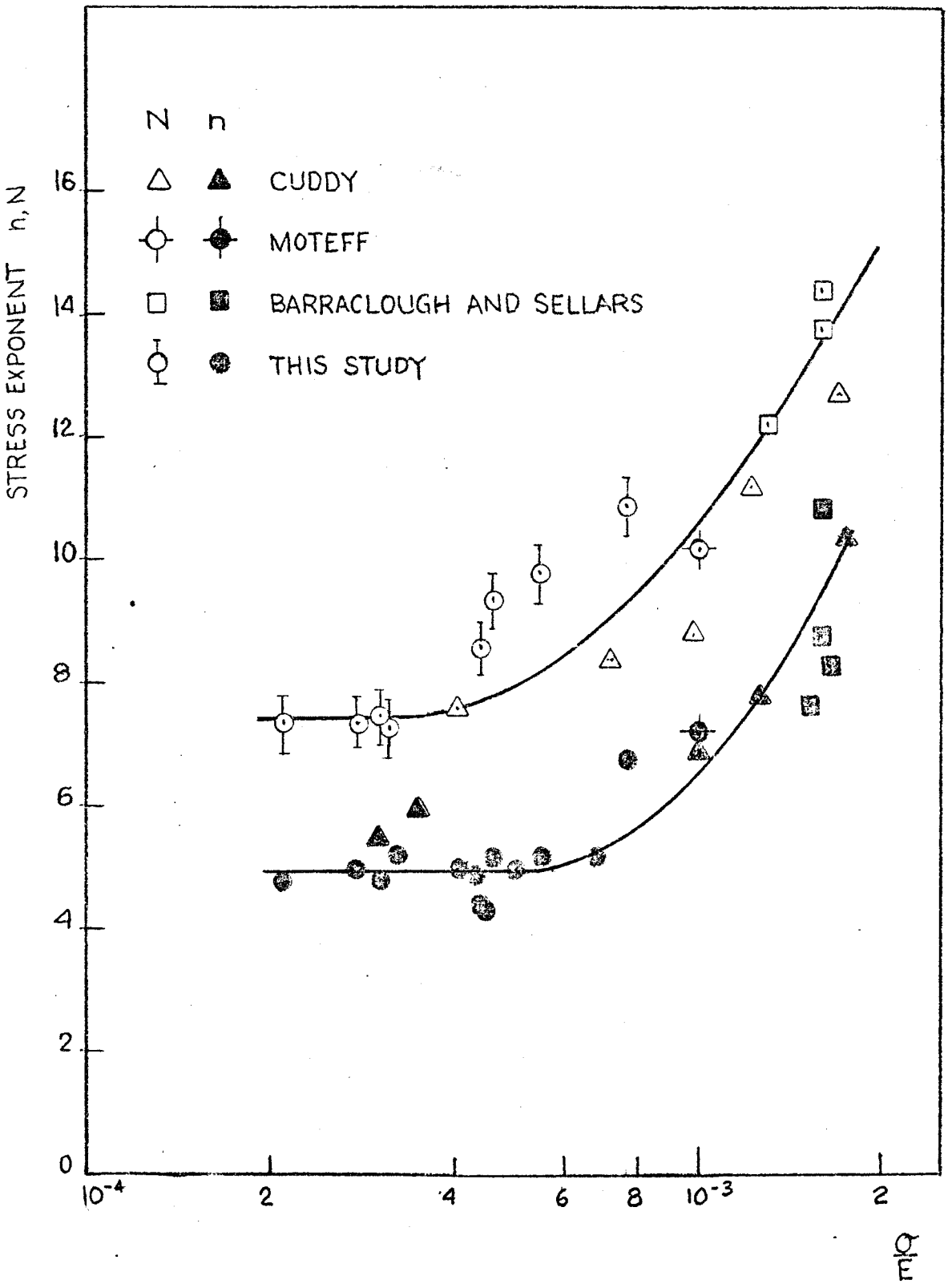

Figure 6. The stress exponent for constant structure, N, and the stress exponent for steady state structure, n, is shown as a function of σ/E for 304 stainless steel.

is gratifying to note that the data for 304 stainless steel fit in rather well into a common pattern as obtained from the different investigations.

DISCUSSION

The type of results we have obtained for stainless steel coupled with the data reported by others, suggest that the creep resistance of 304 stainless steel can be improved by subgrain size refinement. The type of transient observed in 304 stainless steel is typical of a subgrain strengthened material and parallels closely the behavior of polycrystalline aluminum[7]. A way of analyzing the influence of subgrain size on the strength of stainless steel is to rewrite equation (1) solving for the flow stress at constant strain rate. Thus,

$$\sigma\Big|_{\dot{\varepsilon}} = S' \lambda^{-p/N} \qquad (7)$$

where $S' = (\frac{\dot{\varepsilon}}{S})^{1/N}$. Thus the flow stress is seen to have a power relation with the subgrain size with an exponent equal to $\frac{p}{N}$. In Figure 7 we illustrate the values of $\frac{p}{N}$, as a function of σ/E, for 304 stainless steel. These results reveal that $\frac{p}{N}$ is about a constant equal to 0.35. This value is approximately the same as that observed for polycrystalline pure aluminum ($\frac{p}{N} = 0.43$). One should note the similarity of our relation to the Hall-Petch equation, $\sigma = \sigma_o + kyd^{-1/2}$. Here σ_o and ky are material constants and d is the grain size. We therefore see that the term, p/N in our expression [eq. (6)] can be related to 1/2 in the Hall-Petch relation. Subgrain strengthening at high temperatures apparently exhibits a similar relation to grain boundary strengthening at low temperatures. The predictive aspects of our subgrain size-flow stress relation will be discussed in greater detail later.

Activation energies for creep were determined for our stainless steel data as well as for other data available in the literature. These are recorded in Table 4. The calculated activation energies for creep are in the order of

Table 4

Stress Exponent and Activation Energy for Steady State Creep of 304 Stainless Steel.

Material	n	Q_c kcal/mol	Temp. °C	Test method	Ref.
19Cr-10Ni-0.05C	6-9	76±7	704-927	constant stress tensile creep $\varepsilon p = 0.15$	Cuddy (1970)[5]
19Cr-10Ni-0.05C	8.5	~85	590-700	constant load creep	Moteff (1971)[8]
18Cr-14Ni-0.004C	5.3	75	650	constant load tensile creep ΔT	Ohta (1970)[9]
19Cr-10Ni-0.08C	7.5	68-85	600-700	constant load tensile creep	NRIM CDS No. 4[1]
18Cr-9Ni-0.06C	4.7	65-88	900-1100	compression	This study
18Cr-11Ni-0.05C	5.95	73-75	950-1165	Torsion	Barraclough & Sellars (4

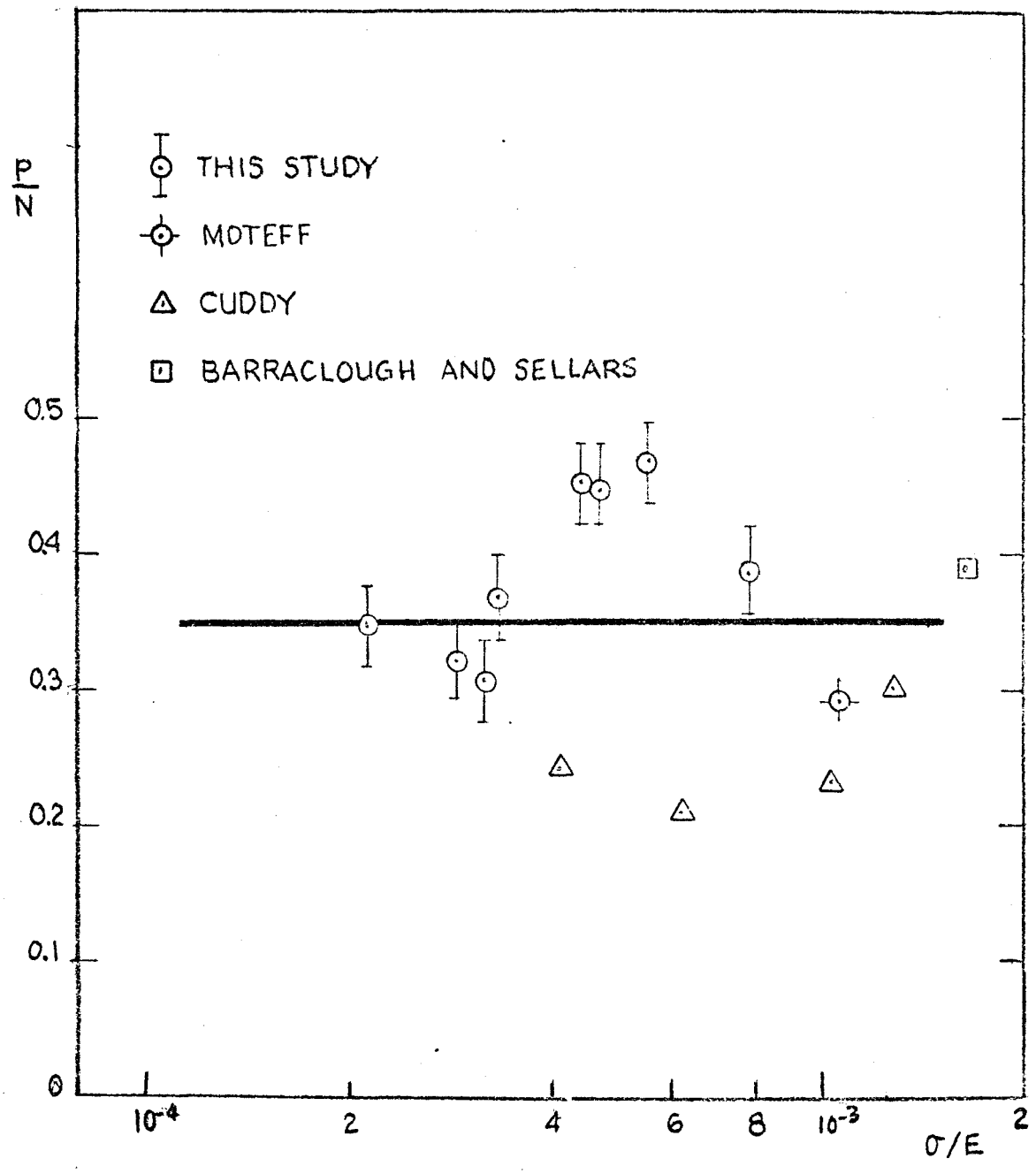

Figure 7. The subgrain strengthening exponent, $\frac{p}{N}$, (in the relation $\sigma = S' \lambda^{-p/N}$) as a function of σ/E for 304 stainless steel. The value of $p/N \approx 0.35$ is in close agreement to that observed for polycrystalline aluminum[7] where $p/N = 0.43$.

75 kcal per mole (± 10 kcal per mole). This value is in the order of, but higher than, the activation energy for lattice self-diffusion in stainless steel (Q_L = 69 kcal per mole).[11] Our calculation of the activation energy for creep was made by taking into account the correction for the modulus variation with temperature. (The modulus-temperature curve is given in Figure 8.) That is, the activation energy was calculated for constant σ/E, and not for constant σ, following the usual expression

$$Q_c\Big|_{\sigma/E} = -R \frac{d\ln \dot{\varepsilon}}{d\ 1/T} \qquad (8)$$

The correction factor for modulus variation with temperature was large and typically about 15-20 kcal per mole. (Without the correction the calculated activation energy for creep is about 90 kcal/mole.) It is not clear why Q_c is somewhat greater than Q_L. One possible explanation is that the stacking fault energy is a function of temperature and this factor is known to influence the creep rate. Data on stacking fault energy variation with temperature, however, are not available for stainless steel. In spite of the lack of exact agreement between Q_c and Q_L it is still likely that atom mobility is the rate controlling process in plastic flow of stainless steel. We point out, for example, that subgrain formation characterizes the microstructure during deformation of 304 stainless steel at warm and hot temperatures; furthermore, its actual creep rate can be reasonably well predicted from the creep behavior of pure metals where diffusion is known to be the rate-controlling process (we expand on this point in the next page and in Figure 10).

In Figure 9 we plot the diffusion compensated strain rate, $\frac{\dot{\varepsilon}}{D_L}$, versus the modulus compensated stress. The lattice diffusion coefficient, D_L, was taken from Perkins, Padgett and Tunali[11]. ($D_L = 0.36 \exp - \frac{68{,}800}{RT}$ cm^2/sec). Data from various investigators are included in the figure.

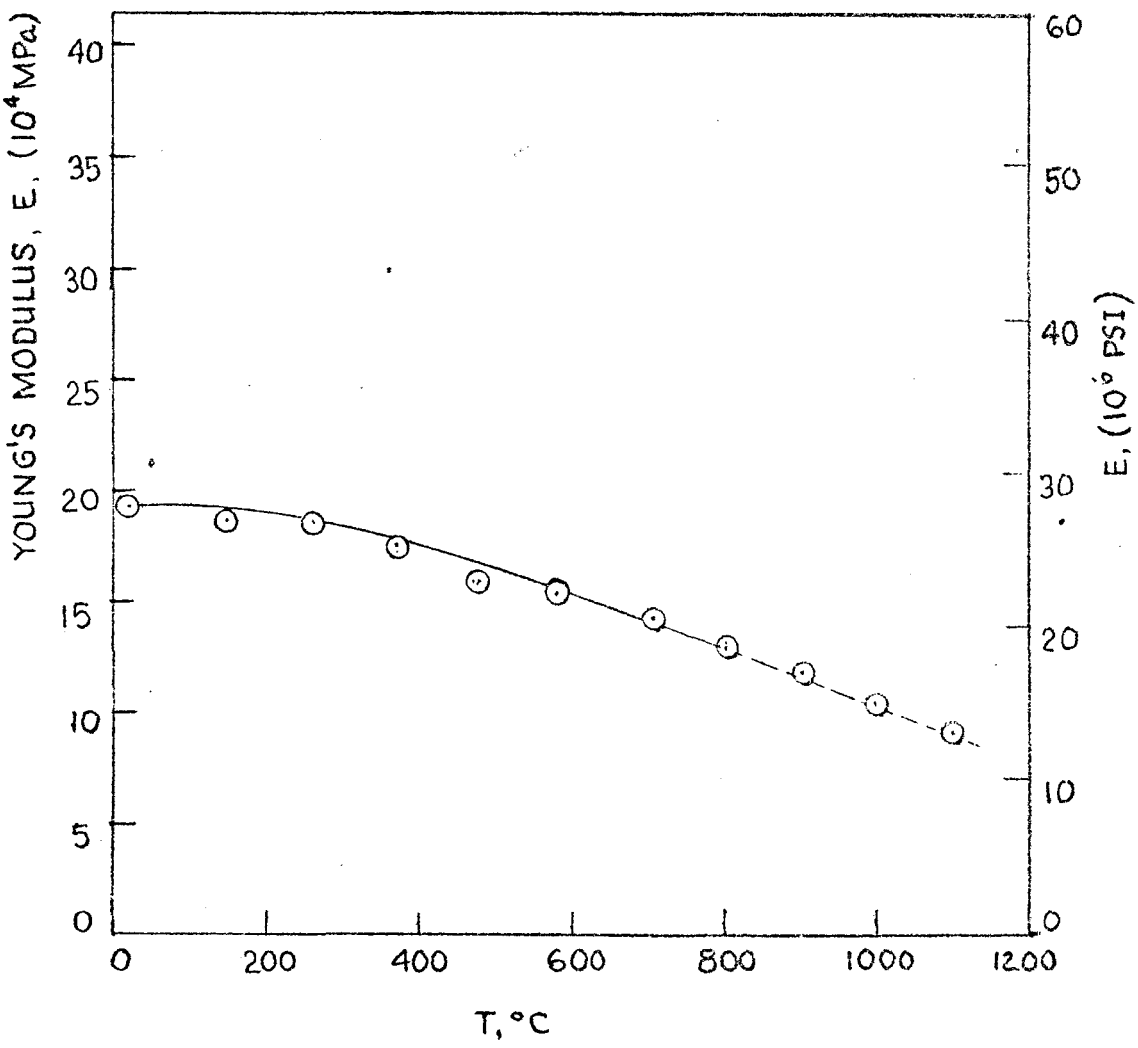

Figure 8. Dynamic Young's modulus for 304 stainless steel as a function of temperature[10].

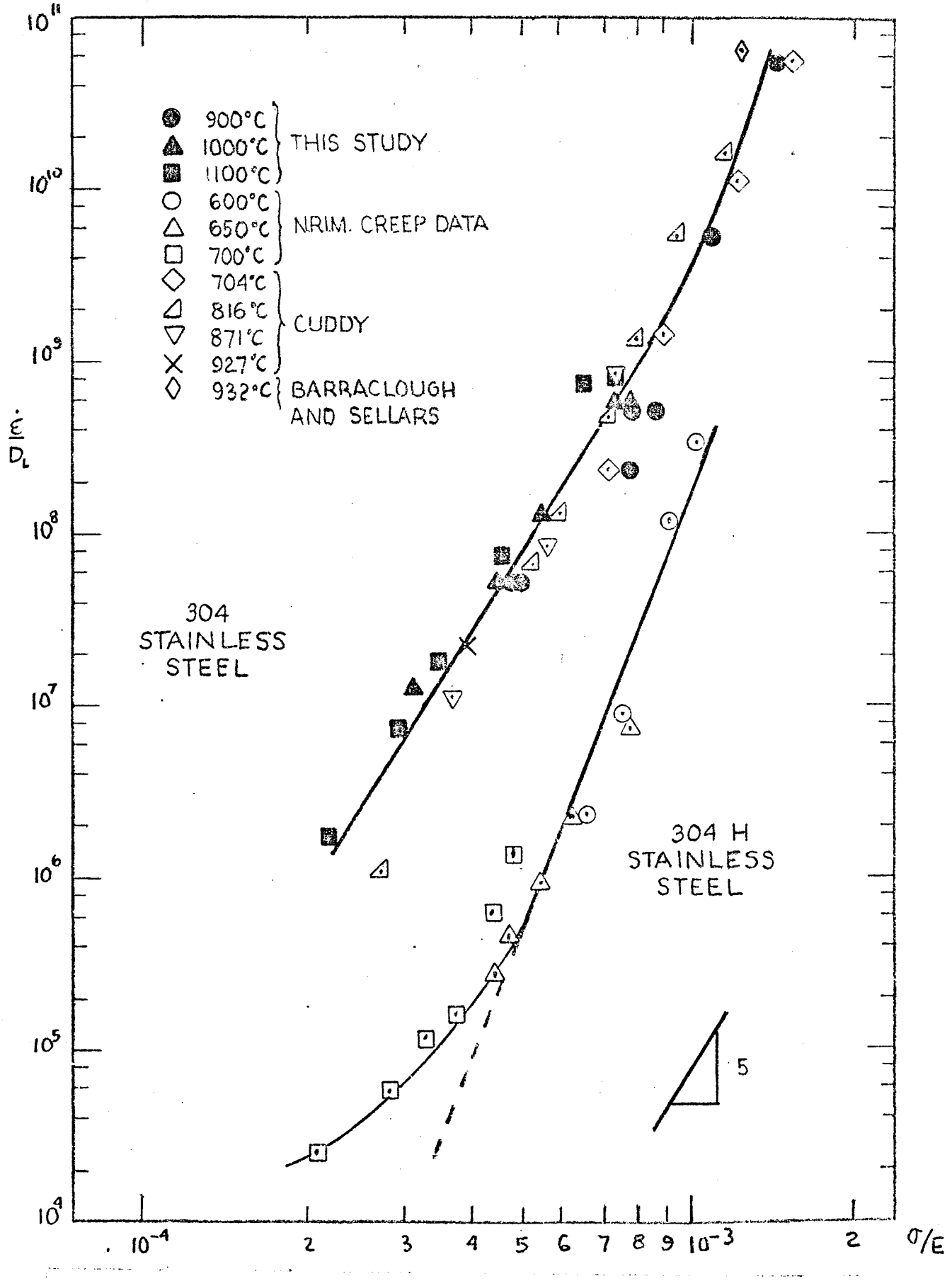

Figure 9. Diffusion compensated creep rate as a function of modulus compensated stress for 304 stainless steel from several investigations.

The compression data from this investigation agrees with the tension data of Cuddy and the torsion data of Barraclough and Sellars. Collectively, these data reveal a power law region with $n \simeq 5$ and power law breakdown at high stresses ($\sigma/E > 10^{-3}$). This behavior is normally observed for most pure metals and many solid solution alloys[6]. The 304H stainless steel is considerably stronger than the other stainless steels. This material is known to contain a fine dispersion of $M_{23}C_6$ carbides; it is possible that fine subgrains are stabilized by the presence of these carbides which results in the high creep resistance observed. In fact, the slope of eight drawn through the data is in agreement with the concept that one is dealing here with constant structure where a value of $N \simeq 7.5$ is expected in the power law region (Figure 6). We hypothesize that the deviation from linearity observed for 304H at low stresses and high temperatures is due to overaging from precipitate coarsening.

The results summarized in Figures 6 and 7 reveal that $\dot{\varepsilon} \propto \lambda^p \sigma^N$ where $p \simeq 2.5$ and $N \simeq 7.5$ in the power law region. The value of p and N are quite similar to the values obtained for pure aluminum where $p \simeq 3.5$ and $N \simeq 7.5$. These observations permit us to write the following equation to describe the steady state creep rate

$$\dot{\varepsilon}_s = S'' \lambda^3 D_L \left(\frac{\sigma}{E}\right)^8 \qquad (9)$$

where S" is a constant principally a function of the stacking fault energy. In order to determine if the stainless steel studied fits into the general behavior observed for other metals[12] we plot $\frac{\dot{\varepsilon}_s}{D_L \lambda^3}$ as a function of the stacking fault energy, for a given value of σ/E, in Figure 10. We note an excellent general trend for 304 stainless steel with the behavior of other metals and alloys. That is, the good correlation shown in Figure 10 attests to the possible importance of subgrain strengthening in creep of 304 stainless steel. If the 304H

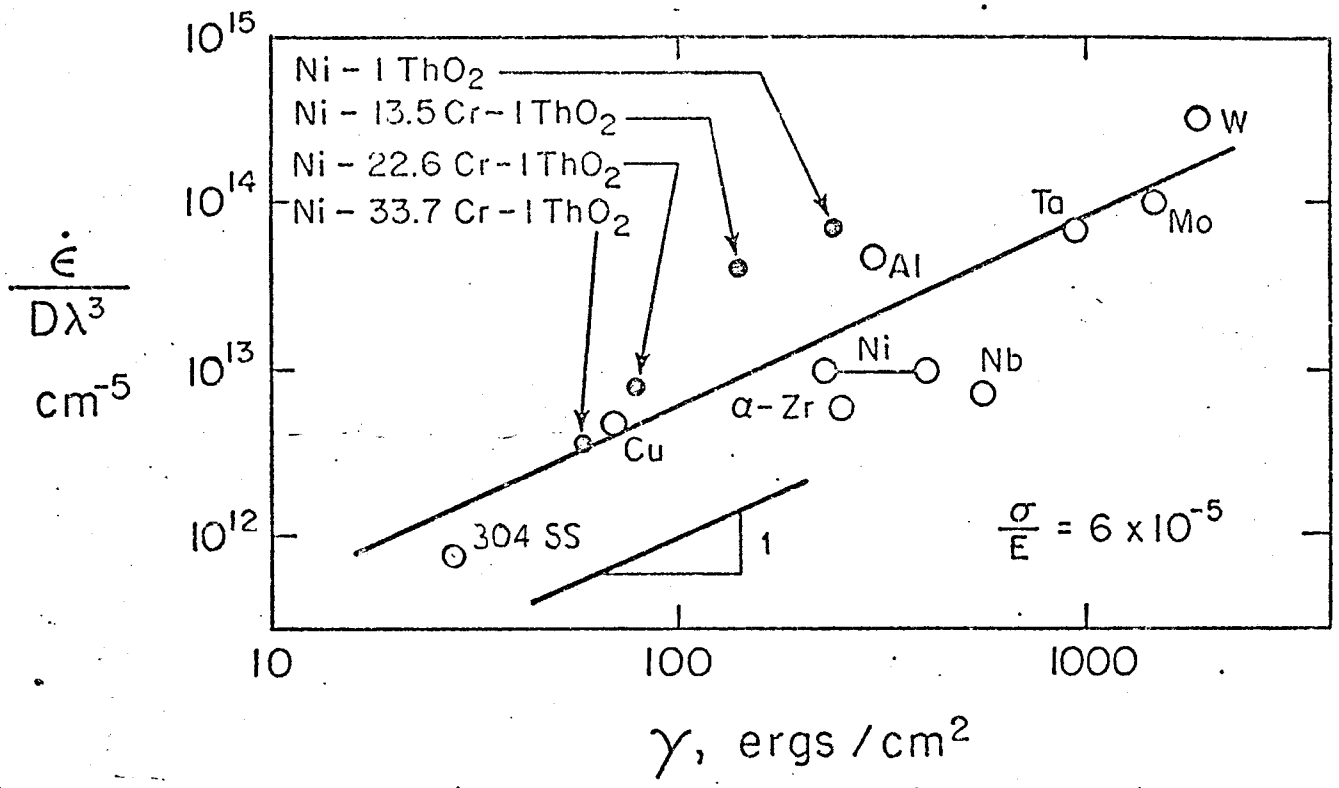

Figure 10. The creep rate of 304 stainless steel is compared with the creep rate of other materials as a function of stacking fault energy after compensating for the diffusion coefficient, subgrain size, stress and modulus. The good correlation obtained attests to the likely important contribution of subgrain size to the creep strength proposed as $\dot{\varepsilon} \propto \lambda^3$ [equation (9)].

stainless steel, shown in Figure 9, is to fit with the creep rate - stacking fault energy curve (Figure 10), a subgrain size of 0.5μm needs to be assigned to characterize its structure. This size is not unreasonable in the light of the fine precipitates contained in the particular stainless steel studied.

It is possible to predict, quantitatively, the strength of 304 stainless steel at any temperature and strain rate from the $\frac{\dot{\varepsilon}}{D_L}$ versus $\frac{\sigma}{E}$ curve of Figure 9 and from equation (7). We do this in Figure 11 where we show the relationship between the strength and the subgrain size for two strain rates. The upper line is for a strain rate of 5×10^{-5} s^{-1} (typical -f the rate for determining yield strengths of metals) and the lower line is for a strain rate of 10^{-10} S^{-1} (a creep rate equivalent to a rupture life of 10,000 hours). The predicted curves are for 650°C a temperature characteristic of the peak operating temperature for fuel cladding elements to be used in the LMFBR. On the same graph we illustrate the equilibrium subgrain size expected at each strain rate and temperature. At $\dot{\varepsilon} = 10^{-10}S^{-1}$, the equilibrium subgrain size is 3.4μm and the accompanying flow stress is 6000 psi. We predict, however, that the flow stress can be increased to 16,000 psi if the subgrain size can be stabilized to 0.2μm. This is the type of objective that faces us in our attempt to develop new heat-resistant materials by novel thermal-mechanical processing methods.

The results described in this report indicate that a high potential of strengthening is possible in 304 stainless steel through subgrain refinement strengthening. Our change-in-strain-rate tests have revealed, however, that the substructure developed in our austenitic steel is not very stable. We made this discovery when we performed decrease-in-strain-rate tests, allowing the load to relax to nearly zero before reapplying the new low strain rate. The resulting stress-strain curve revealed a yield strength that was less than the steady state flow stress for the same low strain rate. Such a test is shown in

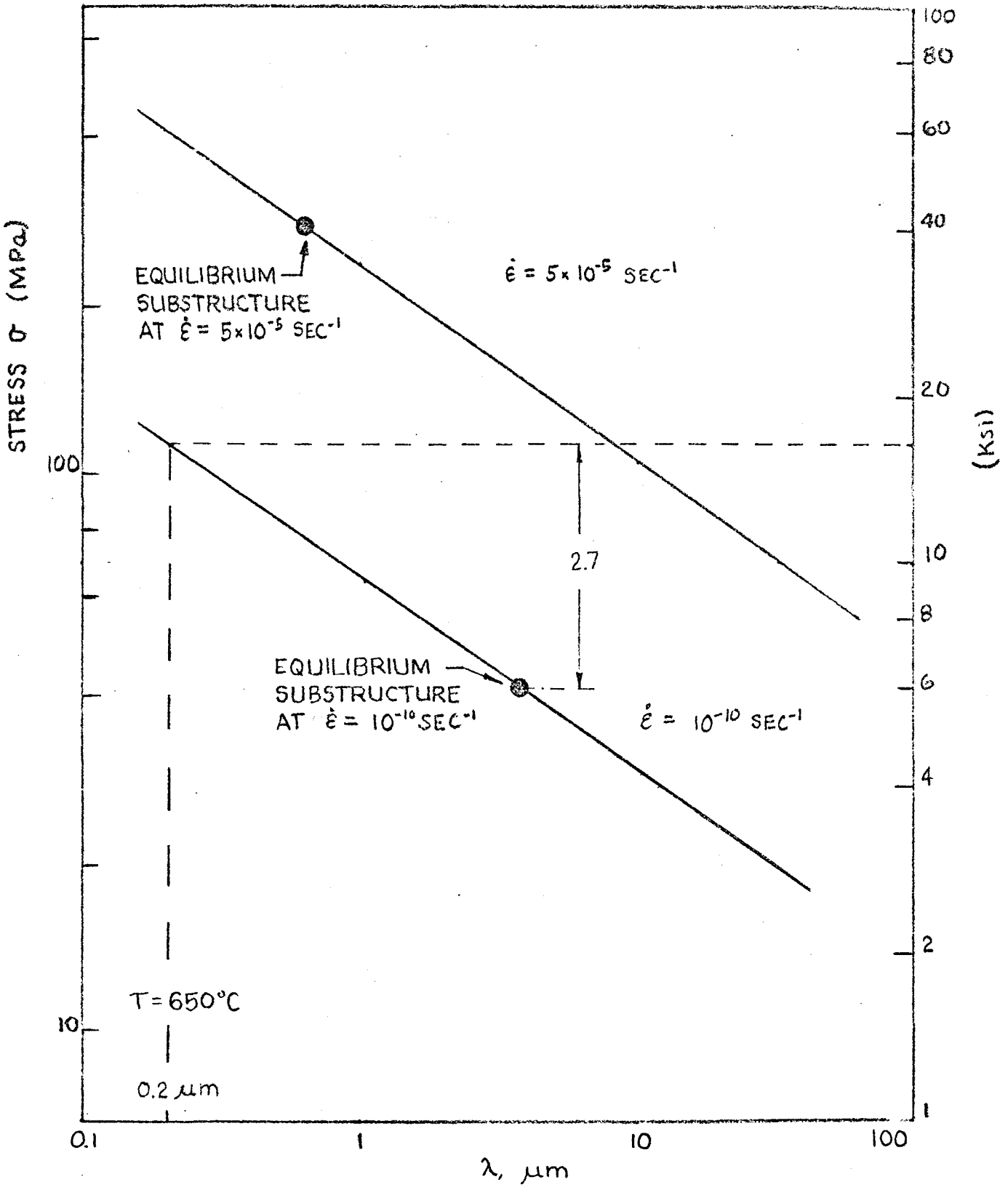

Figure 11. The predicted strength of 304 stainless steel as a function of subgrain size at 650°C for two strain rates. The normal strength of 304 stainless steel can be enhanced by a factor of 2.7 at $\dot{\varepsilon} = 10^{-10}$ secs^{-1} if a stable subgrain size of 0.2μm can be developed.

Figure 12. This result indicates that the substructure apparently readily breaks up when a strain rate is applied that is lower than the strain rate used initially to obtain the substructure [apparently, if the strain rate is changed instantaneously, the new flow stress does reflect the presence of a strong substructure and a high resistance to plastic flow results, (see, for example, our data in Figure 3 and the results of Barraclough and Sellars in Figure 5)]. The results shown in Figure 12 can be explained either by rapid recovery of the substructure at the high temperature of testing (1100°C) or it may be due to a stress accelerated recovery during application of the new low strain rate. Some of our future studies will be devoted to understanding and controlling these apparent instabilities.

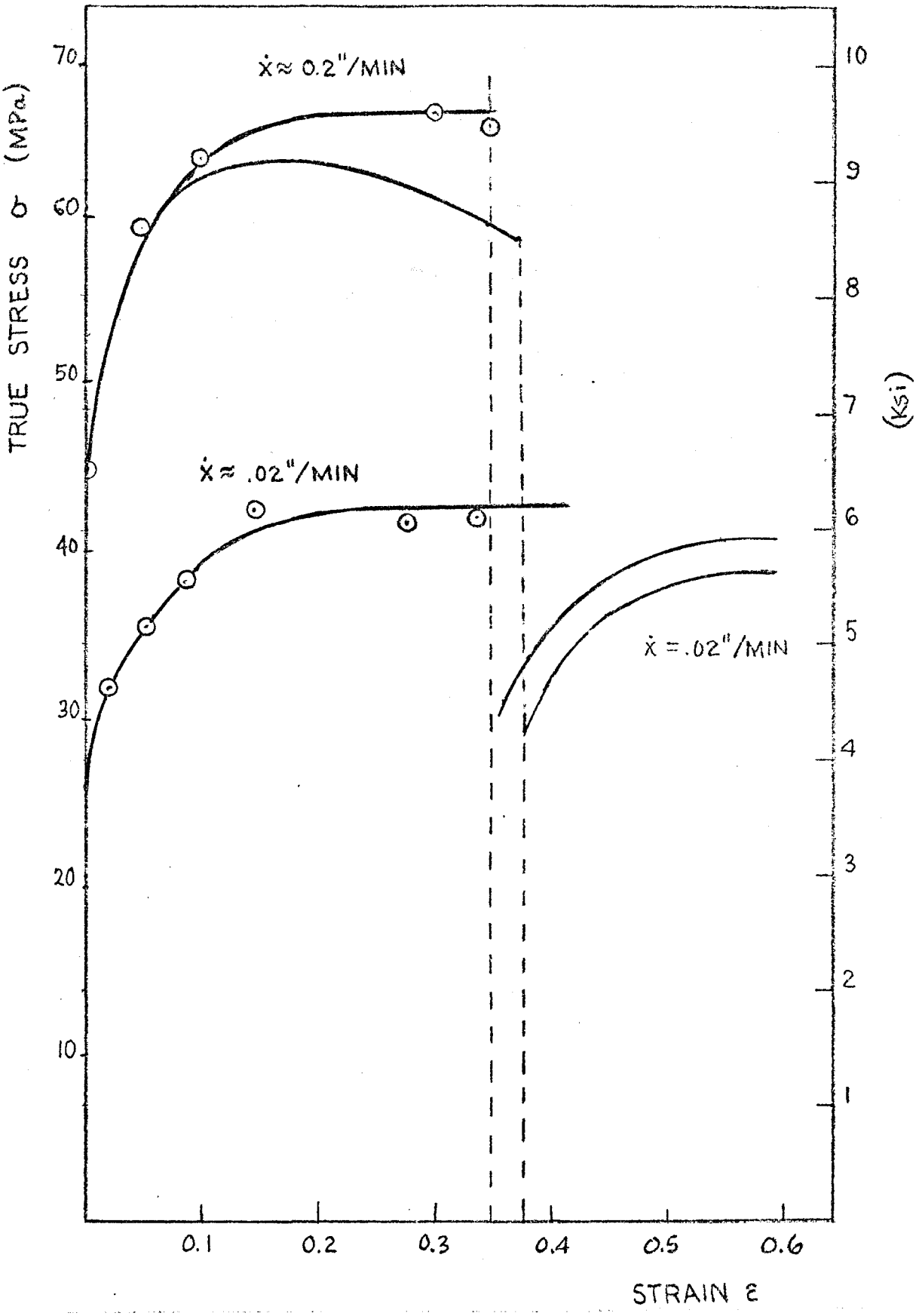

Figure 12. Decrease in strain rate tests performed on 304 stainless steel at 1100°C reveal rapid softening if the stress is reduced to zero stress before application of the new low strain rate.

REFERENCES

1. National Research Institute for Metals, Tokyo, Japan, Creep Data Sheet No. 4, 1972.

2. O. D. Sherby and C. M. Young, Rate Processes in Plastic Deformation, John Dorn Memorial Symposium (Oct. 1973), published by American Society for Metals, Metals Park, Ohio, 1975.

3. C. M. Young and O. D. Sherby, J. Iron and Steel Institute, 211, 640, 1973.

4. D. R. Barraclough and C. M. Sellars, Mechanical Properties at High Rate of Strain, International Conference, Oxford, April 1974, J. Harding, editor, Institute of Physics, London.

5. L. J. Cuddy, Metallurgical Transactions, 1, 395, 1970.

6. O. D. Sherby and P. M. Burke, Prog. Mats. Sci., 13, 325, 1968.

7. C. M. Young, S. L. Robinson and O. D. Sherby, Acta Met., 23, 633, 1975.

8. J. Moteff, Progress Report COO-2107-4 USERDA Contract AT (11-1)-2107, October 1971.

9. S. Yamamoto and S. Ohta, Research and Development, Kobe Steel, 20, 21 1970.

10. F. Garofalo, P. R. Malenuck and G. V. Smith, ASTM STP 129, 10-27, June 1952.

11. R. A. Perkins, R. A. Padgett and N. K. Tunali, Metallurgical Transactions, 4, 2535, 1973.

12. S. L. Robinson, Ph.D. Dissertation, Stanford University, Stanford, California, 1972.